Observation of Two Different Oscillation Periods in the Exchange Coupling of Fe/Cr/Fe(100)

J. Unguris, R. J. Celotta, and D. T. Pierce
National Institute of Standards and Technology, Gaithersburg, Maryland 20899
(Received 11 April 1991)

Oscillations of ferromagnetic to antiferromagnetic exchange coupling between two Fe layers separated by a Cr spacer of linearly increasing thickness were investigated by imaging the magnetic domains with scanning electron microscopy with polarization analysis. Up to six oscillations in the coupling with a period of 10–12 Cr layers were observed, and, in the case of an extremely well ordered Cr interlayer, additional oscillations with a period of 2 Cr layers were observed.

PACS numbers: 75.50.Rr, 75.30.Et, 75.70.Cn

Sandwiches and superlattices of Fe/Cr/Fe have recently attracted wide interest because of their exciting properties. The Fe layers were first observed [1] to couple antiferromagnetically for a Cr thickness in the neighborhood of 1 nm and have since been found to exhibit long-range periodic modulation in the antiferromagnetic coupling strength through Cr layers up to 5 nm thick [2]. Moreover, an unusually large reduction in the resistance was found when antiparallel Fe layers are reoriented parallel to an applied magnetic field [3,4]. This "giant" magnetoresistance effect has potentially important technological applications to magnetoresistive recording heads and sensors. The long-range coupling and large magnetoresistance have now been observed on polycrystalline [2] as well as single-crystal [3–5] structures and for a number of other material combinations [2,6,7]. Although there is an increasing body of experimental results, along with theoretical investigations of the coupling [8–10] and the giant magnetoresistance [11,12], our understanding of these phenomena is still incomplete.

This paper focuses on the magnetic interaction between two Fe layers separated by a Cr layer. We have grown well-characterized, epitaxial, single-crystal Fe/Cr/Fe sandwich structures in which the thickness of the Cr layer is continuously varied from 0 to over 10 nm. By using scanning electron microscopy with polarization analysis [13] (SEMPA) we observe directly whether the top Fe layer is ferromagnetically or antiferromagnetically coupled to the bottom layer and accurately determine the Cr thickness at which the coupling reverses. When the crystal quality of the intervening Cr layer is improved, there are additional, previously unobserved, oscillations in the coupling with the period of the Cr lattice constant.

The sample preparation and experiments are carried out in an ultrahigh-vacuum scanning electron microscope capable of scanning Auger microscopy, scanning electron microscopy with polarization analysis, and reflection high-energy electron diffraction (RHEED). The first layer of the sandwich structure is an Fe(100) single-crystal whisker initially cleaned by 2-keV Ar-ion bombardment at 750 °C. The principal contaminant, oxygen, is removed to below the Auger detection limit of about 0.05 monolayer. The Cr is evaporated to form a wedge-shaped spacer layer (see Fig. 1) by moving a precision piezocontrolled shutter during evaporation. The Fe substrate during Cr growth was at either room temperature or elevated temperature. In these and other measurements, short-period oscillations were observed for Cr growth on the Fe substrate at elevated temperatures in the range 200–300 °C. The crystalline quality of the Fe substrate, the bare Cr wedge, and the 2-nm-thick Fe overlayer were checked with RHEED. The wedge area was typically a few hundred μm wide by a few hundred μm long with a maximum thickness of 5 to 20 nm. The high spatial resolution of the SEM allows us to use the small, nearly perfect Fe single-crystal whisker substrate. The clear advantage of the wedge structure is that it allows measurements at many different thicknesses with a reproducibility in relative thickness that could not be achieved by preparing many individual sandwiches each with a different Cr thickness. A wedge structure has also been used in magneto-optic Kerr-effect studies of Fe/Cr/Fe [14].

The SEMPA measurement produces three simultaneous images: the usual SEM topography image derived from the intensity of the secondary electrons, and images

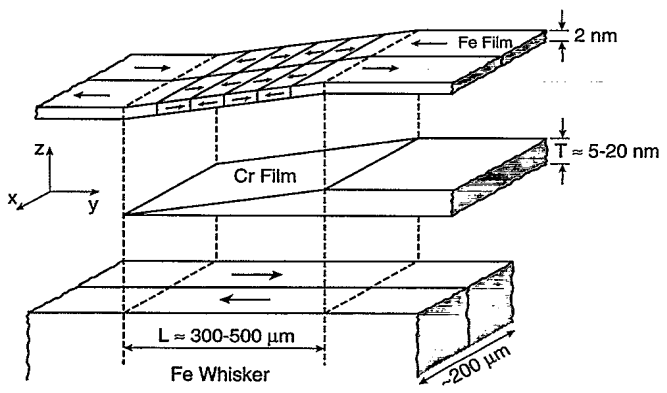

FIG. 1. A schematic exploded view of the sample structure showing the Fe(100) single-crystal whisker substrate, the evaporated Cr wedge, and the Fe overlayer. The arrows in the Fe show the direction of the magnetization in each domain. The z scale is expanded approximately 5000 times; the actual wedge angle is of order 10^{-3} deg.

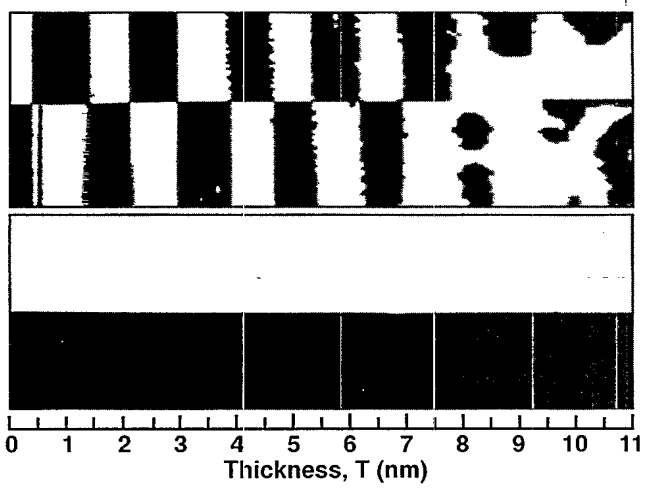

FIG. 2. SEMPA image of the magnetization M_y (axes as in Fig. 1) showing the domains in the clean Fe whisker (lower panel) and in the Fe layer (top panel) covering the room-temperature-evaporated (2.7 ML/min, ML denotes monolayer) Cr wedge which varies linearly in thickness as shown on the bottom scale. Each image represents a region 490 μm long and 280 μm high.

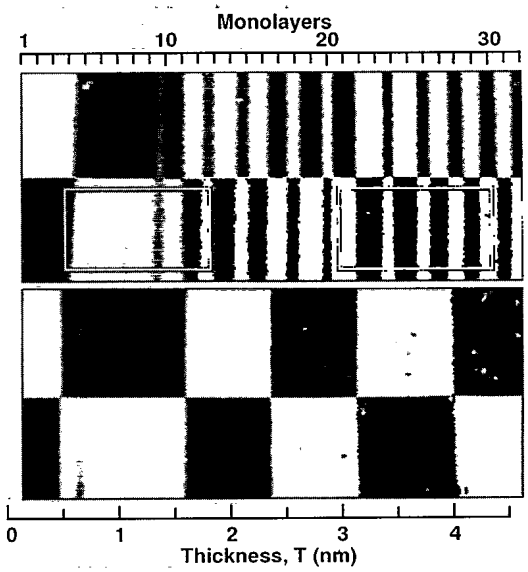

FIG. 3. The difference in the magnetic coupling of the Fe layers in the Fe/Cr/Fe sandwich for the Cr wedge grown (2.7 ML/min) on a substrate at room temperature (lower panel) and grown (7.2 ML/min) on a substrate at elevated temperature (upper panel) is clear in these SEMPA M_y images. The images in the upper and lower panels represent areas 300×280 and 350×290 μm, respectively.

of two vector components of the magnetization from a measurement of the spin polarization of the secondary electrons. For this study, the components of magnetization parallel to the surface of the Fe whisker are measured. The easy axes of magnetization, ⟨100⟩, are the x and y directions, transverse to and along the length of the whisker, respectively. The region of interest on the clean Fe whisker has the simple domain structure shown in the SEMPA image in the lower panel of Fig. 2 and schematically in Fig. 1. There are two domains with only a y component, M_y, of the magnetization along the length of the whisker. In the SEMPA image, the white (black) regions correspond to M_y in the positive (negative) y direction. The domains in the top Fe layer of a Fe/Cr/Fe sandwich for room-temperature evaporation of the Cr wedge are displayed in the top panel of Fig. 2. The thickness of the wedge is zero at the left of the panel and increases linearly over a distance of 490 μm to a thickness of 11 nm at the right edge. The coupling starts off ferromagnetic at small Cr thickness, then changes to antiferromagnetic as the thickness increases, and oscillates in this manner for a startling six periods. The period or wavelength of the oscillations varies between about 1.4 to 1.7 nm, equivalent to the thickness of 10 to 12 Cr layers, with the first antiferromagnetic oscillation longer than the others.

In Fig. 3 we show SEMPA images of the Fe-top-layer magnetization for two different cases of Cr wedge growth. The Cr wedges in the lower panel and upper panel were grown on Fe whisker substrates at room temperature and elevated temperature, respectively. In both cases the initial RHEED pattern for the Fe whisker substrate shows an arc of sharp spots characteristic of a perfect single crystal. The RHEED pattern for the room-temperature-grown Cr exhibited a slight streaking of the spots indicative of some disorder. The streaking was absent in the pattern for the Cr grown at higher temperature which looked as well ordered as the substrate. The difference in the crystalline quality of the Cr layer drastically changes the coupling of the Fe layers as can be seen in the SEMPA magnetization images. The lower panel of Fig. 3 shows the characteristic long-period oscillatory coupling of the Fe through the Cr seen in Fig. 2. In striking contrast, the magnetization in well-ordered Cr shown in the top panel changes to the much shorter period of about two atomic layers (0.288 nm); that is, the magnetization changes with each atomic-layer change in Cr thickness.

We measure the wedge thickness by measuring the variation in the specular RHEED beam intensity as the incident electron beam is scanned along the wedge. This is analogous to the conventional measurement of the oscillation in the specular RHEED intensity as the film thickness changes with time during growth. The measured RHEED intensity oscillations are shown in the top part of Fig. 4. The RHEED oscillations are registered with the SEMPA image by aligning three defects which are manifested both in the RHEED oscillations and in the SEMPA magnetization image of Fig. 3. The variation in M_y, obtained by averaging line scans over the top half of the upper panel of Fig. 3, is displayed in the lower

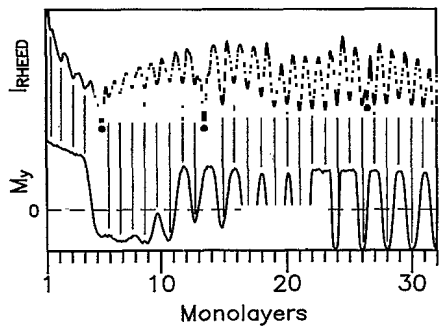

FIG. 4. The positive and negative variations of M_y derived from the upper half of the image in the top panel of Fig. 3 is compared to RHEED intensity oscillations measured by scanning the electron beam across the same region. The solid circles identify defects which allow registry of the RHEED oscillations and the magnetization image. There is an uncertainty of ± 0.5 layer in the zero position of the thickness scales in Figs. 2–4.

part of Fig. 4. The oscillations in M_y line up with the RHEED oscillations except for a "phase slip" of 1 monolayer between 21 and 24 monolayers.

In the *thin part* of the Cr wedge the short-period magnetization angle does not reverse by 180°, as seen in the lower part of Fig. 4, but rotates toward the x direction. In this region, the long-period oscillations are still evident. A rotation of the magnetization into the x direction can be seen clearly in Fig. 5, where 5(a) and 5(b) show M_y from the regions marked in Fig. 3, and 5(c) and 5(d) are the corresponding M_x images of the same regions. In the *thick part* of wedge, where M_y reverses completely with each atomic layer as in Fig. 5(b), it does so by turning continuously in the plane through either the $+x$ or $-x$ direction as seen in the fine-scale domain structure in the M_x image, Fig. 5(d). As is evident from the plot of M_y in Fig. 4 and from Fig. 5(d), there is a variation in the distance along the Fe whisker over which the transition from $+M_y$ to $-M_y$ takes place, from less than 1 μm for the sharpest transition to about 5 μm for the broader ones.

Our observation of short-period oscillations places additional demands on theories of the magnetic coupling. Since all previous measurements on transition-metal sandwich structures have only seen long-period oscillations, the theoretical effort has been directed toward explaining the long-period oscillations which are unexpected based on experience with RKKY interactions. While Yafet [15] was able to explain the behavior of Gd-Y superlattices with an RKKY interaction, such an explanation is likely to be more problematical for transition-metal sandwiches where the magnetic moments are not localized as in the rare earths. Nevertheless, Wang, Levy, and Fry [8] have calculated the thickness dependence of the coupling for a Fe/Cr/Fe structure using an RKKY-like indirect exchange induced by the mixing of the conduction electrons of Cr with Fe d states. Their

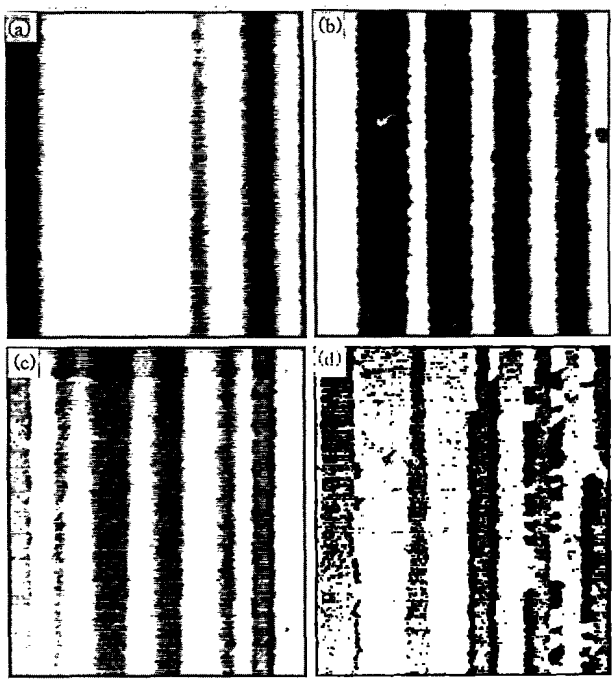

FIG. 5. M_y images from the outlined areas of Fig. 3 in the thin and thick parts of the sandwich are shown in (a) and (b), respectively, and compared to the corresponding M_x images in (c) and (d), respectively.

calculation yields a short-period oscillatory coupling in remarkable agreement with our experimental results. This oscillatory coupling is due to the Fermi-surface nesting that gives rise to the spin-density wave in bulk Cr. They also showed that introducing a roughness of two layers at each Fe/Cr interface smears the short-period oscillations leaving only the longer-period oscillations. It is hard to differentiate between such an RKKY-like coupling and an explanation where the Fe is locked to the spin-density-wave antiferromagnetism of Cr [16], although the latter explanation does not explain the long-period oscillation for less well-ordered surfaces. We did observe short-period coupling at 473 K which is well above the Néel temperature, $T_N = 311$ K, of bulk Cr. However, the ordering temperature for such a thin-film sandwich system is not known, and the spin-density wave could be stabilized by coupling to the Fe.

The importance of our results is that we see changes in the magnetic coupling with *both* a long and, for a very-well-ordered Cr interlayer, a short period. The short period is consistent with that determined by the Cr Fermi-surface nesting vector. The 1-layer slip in the phase of the alignment of magnetic oscillations and RHEED oscillations after 21 to 24 layers is consistent with a Fermi-surface wave vector 4% different from the lattice wave vector [16]. In the upper panel of Fig. 3 it is apparent that the long-period oscillations are visible for thinner regions of the Cr. If one pictures the measured

results as arising from a superposition of interactions, one of long and one of short period, the data from the sandwich with the Cr wedge grown at elevated temperature suggest that the relative amplitude of the long-period to short-period interaction decreases with increasing Cr thickness. If both the long- and short-period oscillations are RKKY-like, the slower falloff in the envelope of the short-period oscillations is consistent with their deriving from the special situation of nesting Fermi surfaces [17].

We have benefited greatly from very helpful discussions with M. Stiles. The experimental contribution of M. Hart during the apparatus development is greatly appreciated. Useful discussions with J. Fry, F. Herman, and P. Levy are gratefully acknowledged. The Fe whiskers kindly provided by A. Arrott were grown at the Simon Fraser University under an operating grant from the National Science and Engineering Research Council of Canada. This work was supported in part by the Office of Naval Research.

Note added.—Since the submission of this paper, we have received preprints describing the optical observation of the short-period oscillations [18].

[1] P. Grünberg, R. Schreiber, Y. Pang, M. B. Brodsky, and H. Sowers, Phys. Rev. Lett. **57**, 2442 (1986).

[2] S. S. P. Parkin, N. More, and K. P. Roche, Phys. Rev. Lett. **64**, 2304 (1990).

[3] M. N. Baibich, J. M. Broto, A. Fert, F. Nguyen Van Dau, F. Petroff, P. Etienne, G. Creuzet, A. Friederich, and J. Chazelas, Phys. Rev. Lett. **61**, 2472 (1988).

[4] G. Binasch, P. Grünberg, F. Saurenbach, and W. Zinn, Phys. Rev. B **39**, 4828 (1989).

[5] J. J. Krebs, P. Lubitz, A. Chaiken, and G. A. Prinz, Phys. Rev. Lett. **63**, 1645 (1989).

[6] A. Cebollada, J. L. Martínez, J. M. Gallego, J. J. de Miguel, R. Miranda, S. Ferrer, F. Batallán, G. Fillion, and J. P. Rebouillat, Phys. Rev. B **39**, 9726 (1989).

[7] B. Heinrich, Z. Celinski, J. F. Cochran, W. B. Muir, J. Rudd, Q. M. Zhong, A. S. Arrott, K. Myrtle, and J. Kirschner, Phys. Rev. Lett. **64**, 673 (1990).

[8] Y. Wang, P. M. Levy, and J. L. Fry, Phys. Rev. Lett. **65**, 2732 (1990).

[9] D. M. Edwards, J. Mathon, R. B. Muniz, and M. S. Phan (to be published).

[10] H. Hasegawa, Phys. Rev. B **42**, 2368 (1990).

[11] R. E. Camley and J. Barnás, Phys. Rev. Lett. **63**, 664 (1989).

[12] P. M. Levy, K. Ounadjela, S. Zhang, Y. Wang, C. B. Sommers, and A. Fert, J. Appl. Phys. **67**, 5914 (1990).

[13] M. R. Scheinfein, J. Unguris, M. H. Kelley, D. T. Pierce, and R. J. Celotta, Rev. Sci. Instrum. **61**, 2501 (1990).

[14] M. Rührig, R. Schäfer, A. Hubert, R. Mosler, J. A. Wolf, S. Demokritov, and P. Grünberg, Phys. Status Solidi (a) **125** (to be published); S. Demokritov, J. A. Wolf, and P. Grünberg (to be published).

[15] Y. Yafet, J. Appl. Phys. **61**, 4058 (1987).

[16] E. Fawcett, Rev. Mod. Phys. **60**, 209 (1988).

[17] L. M. Roth, H. J. Zeiger, and T. A. Kaplan, Phys. Rev. **149**, 519 (1966).

[18] S. T. Purcell, W. Folkerts, M. T. Johnson, N. W. E. McGee, K. Jager, J. aan de Stegge, W. B. Zeper, and W. Hoving (to be published); S. Demokritov, J. A. Wolf, P. Grünberg, and W. Zinn, in Proceedings of the Materials Research Society Spring Symposium, 1991 (to be published).